Centrality Dependence of the Charged-Particle Multiplicity Density at Midrapidity in Pb-Pb Collisions at $\sqrt{s_{NN}} = 5.02$ TeV

J. Adam *et al.*[*]
(ALICE Collaboration)

(Received 18 December 2015; published 3 June 2016)

The pseudorapidity density of charged particles, $dN_{\mathrm{ch}}/d\eta$, at midrapidity in Pb-Pb collisions has been measured at a center-of-mass energy per nucleon pair of $\sqrt{s_{NN}} = 5.02$ TeV. For the 5% most central collisions, we measure a value of 1943 ± 54. The rise in $dN_{\mathrm{ch}}/d\eta$ as a function of $\sqrt{s_{NN}}$ is steeper than that observed in proton-proton collisions and follows the trend established by measurements at lower energy. The increase of $dN_{\mathrm{ch}}/d\eta$ as a function of the average number of participant nucleons, $\langle N_{\mathrm{part}} \rangle$, calculated in a Glauber model, is compared with the previous measurement at $\sqrt{s_{NN}} = 2.76$ TeV. A constant factor of about 1.2 describes the increase in $dN_{\mathrm{ch}}/d\eta$ from $\sqrt{s_{NN}} = 2.76$ to 5.02 TeV for all centrality classes, within the measured range of 0%–80% centrality. The results are also compared to models based on different mechanisms for particle production in nuclear collisions.

DOI: 10.1103/PhysRevLett.116.222302

The theory describing the strong interaction, quantum chromodynamics (QCD), predicts the existence of a deconfined phase of matter, the quark-gluon plasma, at high temperature and energy density. Ultrarelativistic collisions of nuclei achieve the conditions necessary for the formation of this strongly interacting matter [1,2].

The multiplicity of produced particles is an important property of the collisions related to the collision geometry, the initial parton densities, and the energy density produced. Its dependence on the impact parameter is sensitive to the interplay between particle production from hard and soft processes and coherence effects between individual nucleon-nucleon scatterings. With an increase in the collision energy, the role of hard processes, i.e., parton scatterings with large momentum transfer, increases. After a two-year-long shutdown, the Large Hadron Collider (LHC) restarted operation in June 2015 and produced Pb-Pb collisions at a per nucleon center-of-mass energy of $\sqrt{s_{NN}} = 5.02$ TeV in November 2015. This is the highest energy achieved in the laboratory to date and offers the possibility to further constrain particle production models by studying their $\sqrt{s_{NN}}$ dependence.

Collisions of extended objects such as nuclei can be classified according to their centrality, which is related to the overlap area of the nuclei. This results in different numbers of nucleons participating in the collision. The number of these participants, N_{part}, can be calculated by a Monte Carlo (MC) sampling technique in the Glauber model [3].

Previous measurements of $dN_{\mathrm{ch}}/d\eta$ for nucleus-nucleus (AA) collisions were performed at the LHC by ALICE [4], ATLAS [5], and CMS [6] at $\sqrt{s_{NN}} = 2.76$ TeV and at lower energies, in the range $\sqrt{s_{NN}} = 9$–200 GeV, with experiments at the Super Proton Synchrotron (SPS) and Relativistic Heavy Ion Collider (RHIC) [7–12]. They show that the increase of $dN_{\mathrm{ch}}/d\eta$ with energy is steeper in nucleus-nucleus compared to proton-proton collisions. The centrality dependence of $(2/\langle N_{\mathrm{part}} \rangle)\langle dN_{\mathrm{ch}}/d\eta \rangle$ in Pb-Pb at $\sqrt{s_{NN}} = 2.76$ TeV is very similar to that measured in $\sqrt{s_{NN}} = 200$ GeV collisions at RHIC, pointing to a similar mechanism of particle production at the two energies.

In this Letter, we present the measurement of the charged-particle pseudorapidity density averaged in the interval $|\eta| < 0.5$, $\langle dN_{\mathrm{ch}}/d\eta \rangle$, and its centrality dependence. The pseudorapidity is defined by $\eta \equiv -\ln \tan(\theta/2)$, with θ the emission angle of the particle relative to the beam axis. The primary charged particles are defined as prompt particles produced in the collision including all decay products, except products from weak decays of light flavor hadrons and of muons.

The data were recorded with the ALICE detector in November 2015 at $\sqrt{s_{NN}} = 5.02$ TeV. Full details on the ALICE apparatus [13] and its operational performance [14] are given elsewhere. A brief description of the most relevant elements, along with the experimental conditions, follows. The observed interaction rate was around 300 Hz, of which about 25 Hz were from hadronic interactions, the remainder being a background from electromagnetically induced processes. A total of about 10^5 hadronic events are used. The interaction probability per bunch crossing (during which bunches of ions from each beam are arranged to

[*]Full author list given at the end of the article.

be coincident at the ALICE interaction point) was sufficiently small that the chance of two hadronic interactions occurring together, so-called pileup events, was negligible.

The measurement relies on the ALICE inner tracking system, the innermost two layers of which form the silicon pixel detector (SPD). It consists of arrays of pixels arranged with an approximate cylindrical geometry at radii of 3.9 and 7.6 cm covering intervals of $|\eta| < 2.0$ and $|\eta| < 1.4$ for the inner and outer layers, respectively. The SPD is situated in a solenoidal magnet, with its principal axis along the beam line, providing a 0.5 T magnetic field. The interaction trigger is provided by two detectors, V0A and V0C, which consist of arrays of scintillators, covering the full azimuth and more than four units of pseudorapidity, in the ranges $2.8 < \eta < 5.1$ and $-3.7 < \eta < -1.7$, respectively. In all cases, the η coverage refers to collisions at the nominal interaction point. A signal must be present in both V0 detectors to trigger the recording of the interaction. The V0 detectors also provide a signal proportional to the number of charged particles striking them which is used to classify the events into centrality classes, defined in terms of percentiles of the hadronic cross section. In addition, an offline event selection employs the information from two zero degree calorimeters (ZDCs) positioned 112.5 m from the interaction point on either side. Beam background events are removed by using the V0 timing information and the correlation between the sum and the difference of times measured in each of the ZDCs [14].

The analysis is restricted to the 80% most central events. The classification of events into centrality classes is done by using the summed amplitudes of the signals in the V0A and V0C detectors, following the method developed previously [15,16]. The V0 amplitude is fitted with an MC implementation of the Glauber model coupled with a two-component model assuming that the effective number of particle-producing sources is given by $f \times N_{\rm part} + (1-f) \times N_{\rm coll}$, where $N_{\rm part}$ is the number of participating nucleons, $N_{\rm coll}$ is the number of binary nucleon-nucleon collisions, and $f \sim 0.8$ quantifies their relative contributions. The number of particles produced by each source is distributed according to a negative binomial distribution (NBD), parametrized with μ and k, where μ is the mean multiplicity per source and k controls the contribution at high multiplicity. In the Monte Carlo Glauber calculation, the nuclear density for ^{208}Pb is modeled by a Woods-Saxon distribution for a spherical nucleus with a radius of 6.62 ± 0.06 fm and a skin thickness of 0.546 ± 0.010 fm, based on data from low-energy electron-nucleus scattering experiments [17], and a hard-sphere exclusion distance between nucleons of 0.4 ± 0.4 fm. For $\sqrt{s_{NN}} = 5.02$ TeV collisions, an inelastic nucleon-nucleon cross section of 70 ± 5 mb, obtained by interpolation [18], is used. The fit was restricted to a region where the effects of trigger inefficiency and contamination by electromagnetic processes are negligible. The NBD-Glauber fit provides a good description of the observed V0 amplitude in this region, which corresponds to the most central 90% of the cross section. All events in the sample corresponding to 0%–80% of the hadronic cross section are found to have a well-defined primary vertex, extracted by correlating hits in the two SPD layers.

The $dN_{\rm ch}/d\eta$ measurement is performed by using short track segments, termed tracklets [19]. Tracklet candidates are formed using the position of the primary vertex and a pair of hits, one in each SPD layer. For each of the hits in the pair, two angles are determined with respect to the reconstructed interaction vertex, and the angular differences, $\Delta\varphi$ in the bending plane and $\Delta\theta$ in the polar direction, are calculated for each pair of hits. In order to reject candidates produced by the random combination of two hits, tracklets are selected by a cut on the sum of the squares, $\delta^2 = (\Delta\varphi/\sigma_\varphi)^2 + (\Delta\theta/\sigma_\theta)^2 < 1.5$, where $\sigma_\varphi = 60$ mrad and $\sigma_\theta = 25 \sin^2\theta$mrad. This selection effectively allows the reconstruction of charged particles with transverse momentum (p_T) above the 50 MeV/c cutoff determined by particle absorption in the material.

The acceptance region in η depends on the position of the interaction vertex along the beam line, z. Events with $|z| < 7$ cm are used, corresponding to a coverage of $|\eta| < 0.5$ with an approximately constant acceptance.

A correction is needed to account for the acceptance and efficiency of a primary track to generate a tracklet, including the extrapolation to zero p_T, and for the removal of combinatorial background tracklets. This is computed by using simulated data from the HIJING event generator [20] transported through a GEANT3 [21] simulation of ALICE, where the centrality definition is adjusted so that the particle density is similar to that in real data for the same centrality classes. A reweighting of the generator output is performed to reproduce the p_T distributions of inclusive charged hadrons and the relative abundances of pions, protons, kaons, and other strange particles as measured in Pb-Pb collisions at $\sqrt{s_{NN}} = 2.76$ TeV [22–25]. Using results from $\sqrt{s_{NN}} = 2.76$ TeV is justified, because the relative abundances at $\sqrt{s_{NN}} = 2.76$ TeV change very little from those at $\sqrt{s_{NN}} = 200$ GeV. Any variation with the increase in $\sqrt{s_{NN}}$ to 5.02 TeV will be much smaller than the differences between the default and reweighted HIJING simulations, which lead to differences in the results within the systematic uncertainties estimated below.

The correction takes into account any inactive channels present at the time of data taking as well as losses due to physical processes like absorption and scattering, which may result in a charged particle not creating a tracklet. The fractions of active pixels in the inner and outer SPD layers were about 85% and 97.5%, respectively. The estimated combinatorial background amounts to about 18% in the most central (0%–2.5%) and 1% in the most peripheral (70%–80%) centrality classes. A correction of about 2% for

contamination by secondaries from weak decays is applied based on the same simulation.

Several sources of systematic uncertainty were investigated. The centrality determination introduces an uncertainty via the fitting of the V0 amplitude distribution to the hadronic cross section, due to the contamination from electromagnetically induced reactions at small multiplicity. The fraction of the hadronic cross section (10%) at the lowest multiplicity, where the trigger and event selection are not fully efficient and the contamination is non-negligible, was varied by an uncertainty of $\pm 0.5\%$. This uncertainty was estimated by varying NBD-Glauber fitting conditions and by fitting a different centrality estimator, based on the hits in the SPD. The uncertainty from the centrality estimation results in an uncertainty of 0.5% for central 0%–2.5% collisions, increasing in the more peripheral collision classes, reaching 7.5% for the 70%–80% sample, where it is the largest contribution. Conversely, the uncertainty due to the subtraction of the background is largest for the central event sample, where it is about 2%, and becomes smaller as the collisions become more peripheral, amounting to only 0.2% for the 70%–80% event class. This uncertainty is estimated by using an alternative method where fake hits are injected into real events.

All other sources of systematic uncertainty are independent of centrality. The uncertainty resulting from the subtraction of the contamination from weak decays of strange hadrons is estimated, from the tuned MC simulations, to amount to about 0.5% by varying the strangeness content by $\pm 30\%$. The uncertainty due to the extrapolation down to zero p_T is estimated to be about 0.5% by varying the number of particles below the 50 MeV/c low-p_T cutoff by $\pm 30\%$. An uncertainty of 1% for variations in detector acceptance and efficiency was evaluated by carrying out the analysis for different slices of the z position of the interaction vertex distribution and with subsamples in azimuth.

Other effects due to particle composition, background events, pileup, material budget, and tracklet selection criteria were found to be negligible. The final systematic uncertainties assigned to the measurements are the quadratic sums of the individual contributions and range from 2.6% in central 0%–2.5% collisions to 7.6% in 70%–80% peripheral collisions, of which 2.3% and 7.5%, respectively, are centrality dependent and 1.2% are centrality independent.

The results for $\langle dN_{\rm ch}/d\eta \rangle$ are shown in Table I. In order to compare bulk particle production at different energies and in different collision systems, specifically for a direct comparison to pp and $p\bar{p}$ collisions, the charged-particle density is divided by the average number of participating nucleon pairs, $\langle N_{\rm part} \rangle/2$. The $\langle N_{\rm part} \rangle$ values are calculated with an MC-Glauber for centrality classes defined by classifying the events according to their impact parameter and are also listed in Table I. The systematic uncertainty on

TABLE I. The $\langle dN_{\rm ch}/d\eta \rangle$ and $(2/\langle N_{\rm part} \rangle)\langle dN_{\rm ch}/d\eta \rangle$ values measured in $|\eta| < 0.5$ for 11 centrality classes. The values of $\langle N_{\rm part} \rangle$ obtained with the Glauber model are also given. The errors are total uncertainties, the statistical contribution being negligible.

Centrality	$\langle dN_{\rm ch}/d\eta \rangle$	$\langle N_{\rm part} \rangle$	$(2/\langle N_{\rm part} \rangle)\langle dN_{\rm ch}/d\eta \rangle$
0%–2.5%	2035 ± 52	398 ± 2	10.2 ± 0.3
2.5%–5.0%	1850 ± 55	372 ± 3	9.9 ± 0.3
5.0%–7.5%	1666 ± 48	346 ± 4	9.6 ± 0.3
7.5%–10%	1505 ± 44	320 ± 4	9.4 ± 0.3
10%–20%	1180 ± 31	263 ± 4	9.0 ± 0.3
20%–30%	786 ± 20	188 ± 3	8.4 ± 0.3
30%–40%	512 ± 15	131 ± 2	7.8 ± 0.3
40%–50%	318 ± 12	86.3 ± 1.7	7.4 ± 0.3
50%–60%	183 ± 8	53.6 ± 1.2	6.8 ± 0.3
60%–70%	96.3 ± 5.8	30.4 ± 0.8	6.3 ± 0.4
70%–80%	44.9 ± 3.4	15.6 ± 0.5	5.8 ± 0.5

$\langle N_{\rm part} \rangle$ is obtained by independently varying the parameters of the Glauber model within their estimated uncertainties. For the most central 0%–5% collisions, a density of primary charged particles at midrapidity $\langle dN_{\rm ch}/d\eta \rangle = 1943 \pm 54$ was measured and, normalized per participant pair, corresponds to $(2/\langle N_{\rm part} \rangle)\langle dN_{\rm ch}/d\eta \rangle = 10.1 \pm 0.3$. In Fig. 1, this value is compared to the existing data for central Pb-Pb and Au-Au collisions from experiments at the LHC [4–6], RHIC [8–12], and SPS [7]. The data shown are for 0%–5% except for the results from PHOBOS [11] and ATLAS [5], which are for 0%–6%. The dependence of $(2/\langle N_{\rm part} \rangle)\langle dN_{\rm ch}/d\eta \rangle$ on the center-of-mass energy can be fitted with a power law of the form as^b. This gives an exponent, under the assumption of uncorrelated uncertainties, of $b = 0.155 \pm 0.004$. It is a much stronger s dependence than for proton-proton collisions, where a value of $b = 0.103 \pm 0.002$ is obtained from a fit to the same function [28]. The fit results are plotted with their uncertainties shown as shaded bands. The result at $\sqrt{s_{NN}} = 5.02$ TeV confirms the trend established by lower-energy data, since b is not significantly different when the new point is excluded from the fit. It can also be seen in the figure that the values of $(2/\langle N_{\rm part} \rangle)\langle dN_{\rm ch}/d\eta \rangle$ measured by ALICE for p-Pb [18] and PHOBOS for d-Au [11] collisions fall on the curve for proton-proton collisions, indicating that the strong rise in AA is not solely related to the multiple collisions undergone by the participants, since the proton in p-A collisions also encounters multiple nucleons.

The centrality dependence of $(2/\langle N_{\rm part} \rangle)\langle dN_{\rm ch}/d\eta \rangle$ is shown in Fig. 2. The point-to-point centrality-dependent uncertainties are indicated by error bars, whereas the shaded bands show the correlated contributions. The statistical uncertainties are negligible. The data are plotted as a function of $\langle N_{\rm part} \rangle$ and a strong dependence is observed, with $(2/\langle N_{\rm part} \rangle)\langle dN_{\rm ch}/d\eta \rangle$ decreasing by a

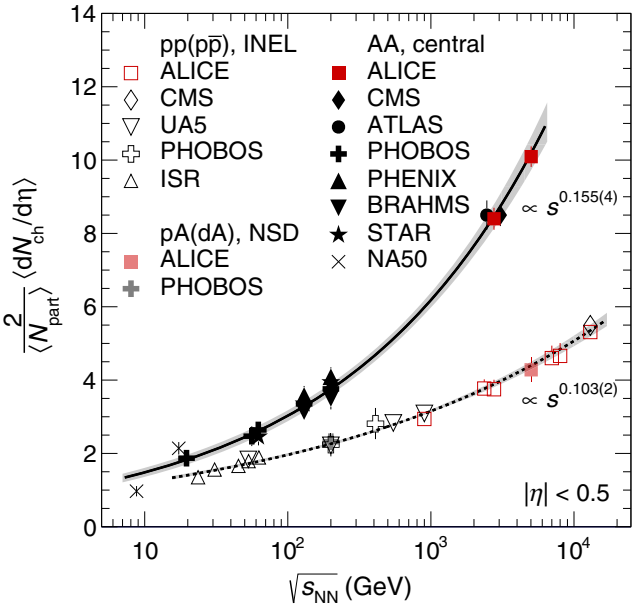

FIG. 1. Values of $(2/\langle N_{\rm part}\rangle)\langle dN_{\rm ch}/d\eta\rangle$ for central Pb-Pb [4–7] and Au-Au [8–12] collisions (see the text) as a function of $\sqrt{s_{NN}}$. Measurements for inelastic pp and $p\bar{p}$ collisions as a function of $\sqrt{s}$ are also shown [26–28] along with those from nonsingle diffractive p-A and d-A collisions [29,30]. The s dependencies of the AA and pp ($p\bar{p}$) collision data are well described by the functions $s_{NN}^{0.155}$ (solid line) and $s_{NN}^{0.103}$ (dashed line), respectively. The shaded bands show the uncertainties on the extracted power-law dependencies. The central Pb-Pb measurements from CMS and ATLAS at 2.76 TeV have been shifted horizontally for clarity.

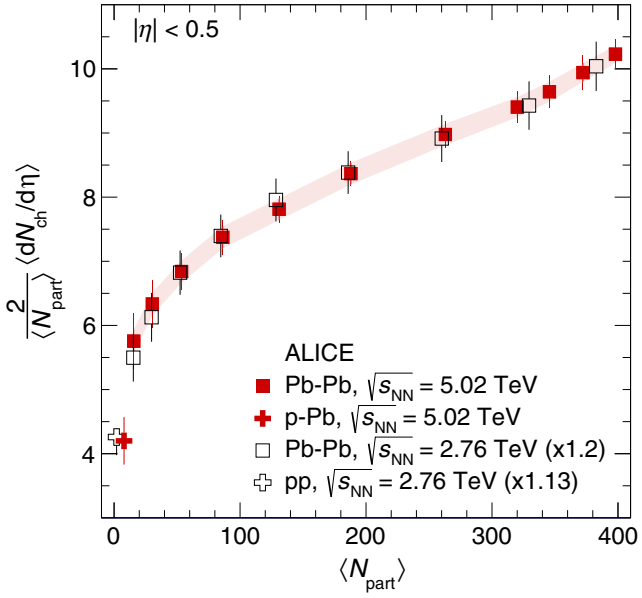

FIG. 2. The $(2/\langle N_{\rm part}\rangle)\langle dN_{\rm ch}/d\eta\rangle$ for Pb-Pb collisions at $\sqrt{s_{NN}} = 5.02$ TeV in the centrality range 0%–80%, as a function of $\langle N_{\rm part}\rangle$ in each centrality class. The error bars indicate the point-to-point centrality-dependent uncertainties, whereas the shaded band shows the correlated contributions. Also shown is the result from nonsingle diffractive p-Pb collisions at the same $\sqrt{s_{NN}}$ [18]. Data from lower-energy (2.76 TeV) Pb-Pb and pp collisions [4,26], scaled by a factor of 1.2 and 1.13, respectively, are shown for comparison. The error bars for p-Pb at $\sqrt{s_{NN}} = 5.02$ TeV and lower-energy Pb-Pb and pp collisions indicate the total uncertainty.

factor of 1.8 from the most central collisions, large $\langle N_{\rm part}\rangle$, to the most peripheral, small $\langle N_{\rm part}\rangle$. There appears to be a smooth trend towards the value measured in minimum bias p-Pb collisions [18]. The Pb-Pb data measured at $\sqrt{s_{NN}} = 2.76$ TeV [4] are also shown, scaled by a factor 1.2, which is calculated from the observed $s^{0.155}$ dependence of the results in the most central collisions and which describes well the increase for all centralities. The proton-proton result at the same energy [26] is scaled by a factor of 1.13 from the $s^{0.103}$ dependence. The ratio between the data measured at the two collision energies is consistent with being independent of $N_{\rm part}$, within the uncertainties, which are largely uncorrelated. While, in general, the uncertainties related to the tracklet measurement are correlated between the two analyses, the subtraction of the background and the centrality classification are, instead, uncorrelated, depending on the determination of the usable fraction of the hadronic cross section and therefore on the run and detector conditions [15].

Figure 3 shows a comparison of the data to some of the models which were compared to the measurements at lower energy. The curves shown are predictions of the models, without any retuning of the parameters based on the new data presented here.

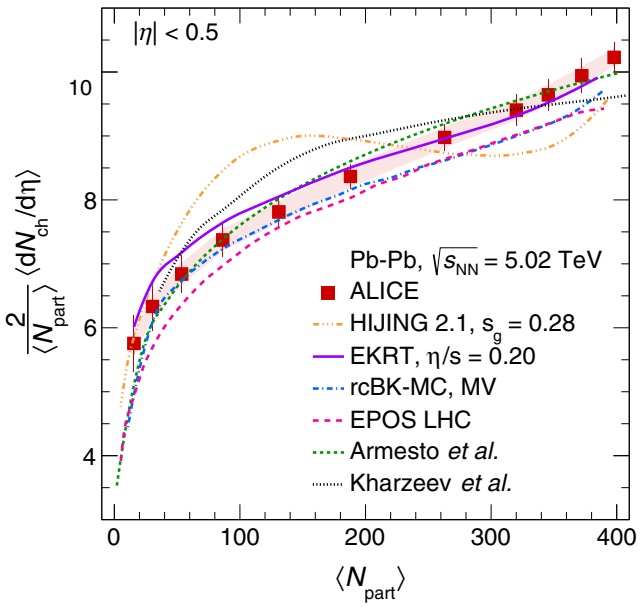

FIG. 3. The $(2/\langle N_{\rm part}\rangle)\langle dN_{\rm ch}/d\eta\rangle$ for Pb-Pb collisions at $\sqrt{s_{NN}} = 5.02$ TeV in the centrality range 0%–80%, as a function of $\langle N_{\rm part}\rangle$ in each centrality class, compared to model predictions [31–39].

Predictions from commonly used Monte Carlo generators, HIJING [33] and EPOS LHC [39], are also shown. HIJING combines perturbative-QCD (pQCD) processes with soft interactions and includes a strong impact parameter dependence of parton shadowing. The data at $\sqrt{s_{NN}} = 2.76$ TeV were previously compared to HIJING using gluon shadowing parameter, s_g, values of 0.20 and 0.23 [4]. The higher value gave a better estimate of the overall normalization, the lower one a better agreement with the shape. At $\sqrt{s_{NN}} = 5.02$ TeV, a larger s_g value of 0.28 is required to limit the multiplicity per participant, leading to a centrality dependence which does not reproduce the data. EPOS is a model based on the Gribov-Regge theory at the parton level which incorporates collective effects treated via a flow parametrization in the EPOS LHC version. It provides a good description of the data.

Saturation-inspired models (rcBK-MC, with the MV initial conditions [35,36], Kharzeev, Levin, and Nardi [38] and Armesto, Salgado, and Wiedemann [37]) rely on pQCD and use an initial-state gluon density to fix an energy-dependent scale at which the quark and gluon densities saturate, thereby limiting the number of produced partons and, in turn, of particles. This results in a factorization of the energy and centrality dependences of the multiplicity in the models, as observed in the experimental data. The rcBK-MC and Armesto, Salgado, and Wiedemann models provide a better description of the data, in particular of the shape, than the Kharzeev, Levin, and Nardi model.

The EKRT model [31,32] combines collinearly factorized next-to-leading-order pQCD minijet cross sections with a conjecture of gluon saturation to suppress soft parton production. Impact-parameter-dependent EPS09s parton distribution functions [40] are used. The space-time evolution of the system with the computed initial conditions is described with relativistic viscous hydrodynamics event by event. The normalization is fixed by exploiting the 0%–5% most central multiplicity measurement [19]. The EKRT model can broadly describe both the shape and the overall magnitude of the dependence of multiplicity on centrality. In general, theoretical models need some sort of mechanism to limit the growth of multiplicity in order to describe the centrality and energy evolution of the multiplicity.

In summary, we have measured the charged-particle pseudorapidity density $\langle dN_{\rm ch}/d\eta \rangle$ in Pb-Pb collisions at the highest available center-of-mass energy and observe a 20% increase for the most central collisions with respect to similar measurements at 2.76 TeV, in agreement with the previously established power-law dependence of this quantity. The centrality dependence of $dN_{\rm ch}/d\eta$ is very similar to that previously measured in lower-energy AA collisions, with a factor of 1.8 increase from peripheral to central collisions. Most of the models which were able to reproduce the data at $\sqrt{s_{NN}} = 2.76$ TeV are able to describe the data at $\sqrt{s_{NN}} = 5.02$ TeV. Our results provide further constraints for models describing high-energy heavy-ion collisions.

The ALICE Collaboration would like to thank all its engineers and technicians for their invaluable contributions to the construction of the experiment and the CERN accelerator teams for the outstanding performance of the LHC complex. The ALICE Collaboration gratefully acknowledges the resources and support provided by all Grid centres and the Worldwide LHC Computing Grid (WLCG) Collaboration. The ALICE Collaboration acknowledges the following funding agencies for their support in building and running the ALICE detector: State Committee of Science, World Federation of Scientists (WFS), and Swiss Fonds Kidagan, Armenia; Conselho Nacional de Desenvolvimento Científico e Tecnológico (CNPq), Financiadora de Estudos e Projetos (FINEP), and Fundação de Amparo à Pesquisa do Estado de São Paulo (FAPESP); National Natural Science Foundation of China (NSFC), the Chinese Ministry of Education (CMOE), and the Ministry of Science and Technology of China (MSTC); Ministry of Education and Youth of the Czech Republic; Danish Natural Science Research Council, the Carlsberg Foundation, and the Danish National Research Foundation; The European Research Council under the European Community's Seventh Framework Programme; Helsinki Institute of Physics and the Academy of Finland; French CNRS-IN2P3, the "Region Pays de Loire," "Region Alsace," "Region Auvergne," and CEA, France; German Bundesministerium fur Bildung, Wissenschaft, Forschung und Technologie (BMBF) and the Helmholtz Association; General Secretariat for Research and Technology, Ministry of Development, Greece; National Research, Development and Innovation Office (NKFIH), Hungary; Department of Atomic Energy and Department of Science and Technology of the Government of India; Istituto Nazionale di Fisica Nucleare (INFN) and Centro Fermi—Museo Storico della Fisica e Centro Studi e Ricerche "Enrico Fermi," Italy; Japan Society for the Promotion of Science (JSPS) KAKENHI and MEXT, Japan; Joint Institute for Nuclear Research, Dubna; National Research Foundation of Korea (NRF); Consejo Nacional de Cienca y Tecnologia (CONACYT), Direccion General de Asuntos del Personal Academico (DGAPA), México, Amerique Latine Formation academique—European Commission (ALFA-EC) and the EPLANET Program (European Particle Physics Latin American Network); Stichting voor Fundamenteel Onderzoek der Materie (FOM) and the Nederlandse Organisatie voor Wetenschappelijk Onderzoek (NWO), Netherlands; Research Council of Norway (NFR); National Science Centre, Poland; Ministry of National Education/Institute for Atomic Physics and National Council of Scientific Research in Higher Education (CNCSI-UEFISCDI), Romania; Ministry of Education and Science of Russian Federation, Russian Academy of Sciences, Russian

Federal Agency of Atomic Energy, Russian Federal Agency for Science and Innovations, and The Russian Foundation for Basic Research; Ministry of Education of Slovakia; Department of Science and Technology, South Africa; Centro de Investigaciones Energeticas, Medioambientales y Tecnologicas (CIEMAT), E-Infrastructure shared between Europe and Latin America (EELA), Ministerio de Economía y Competitividad (MINECO) of Spain, Xunta de Galicia (Consellería de Educación), Centro de Aplicaciones Tecnolgicas y Desarrollo Nuclear (CEADEN), Cubaenergía, Cuba, and IAEA (International Atomic Energy Agency); Swedish Research Council (VR) and Knut and Alice Wallenberg Foundation (KAW); Ukraine Ministry of Education and Science; United Kingdom Science and Technology Facilities Council (STFC); the United States Department of Energy, the United States National Science Foundation, the State of Texas, and the State of Ohio; Ministry of Science, Education and Sports of Croatia and Unity through Knowledge Fund, Croatia; Council of Scientific and Industrial Research (CSIR), New Delhi, India; and Pontificia Universidad Católica del Perú.

[1] F. Karsch, Lattice QCD at high temperature and density, Lect. Notes Phys. **583**, 209 (2002).

[2] B. Muller, J. Schukraft, and B. Wyslouch, First results from Pb + Pb collisions at the LHC, Annu. Rev. Nucl. Part. Sci. **62**, 361 (2012).

[3] M. L. Miller, K. Reygers, S. J. Sanders, and P. Steinberg, Glauber modeling in high-energy nuclear collisions, Annu. Rev. Nucl. Part. Sci. **57**, 205 (2007).

[4] K. Aamodt *et al.* (ALICE Collaboration), Centrality Dependence of the Charged-Particle Multiplicity Density at Midrapidity in Pb-Pb Collisions at $\sqrt{s_{\mathrm{NN}}} = 2.76$ TeV, Phys. Rev. Lett. **106**, 032301 (2011).

[5] G. Aad *et al.* (ATLAS Collaboration), Measurement of the centrality dependence of the charged particle pseudorapidity distribution in lead-lead collisions at $\sqrt{s_{\mathrm{NN}}} = 2.76$ TeV with the ATLAS detector, Phys. Lett. B **710**, 363 (2012).

[6] S. Chatrchyan *et al.* (CMS Collaboration), Dependence on pseudorapidity and on centrality of charged hadron production in PbPb collisions at $\sqrt{s_{\mathrm{NN}}} = 2.76$ TeV, J. High Energy Phys. 08 (2011) 141.

[7] M. C. Abreu *et al.* (NA50 Collaboration), Scaling of charged particle multiplicity in Pb-Pb collisions at SPS energies, Phys. Lett. B **530**, 43 (2002).

[8] I. G. Bearden *et al.* (BRAHMS Collaboration), Charged particle densities from Au + Au collisions at $\sqrt{s_{NN}} = 130$ GeV, Phys. Lett. B **523**, 227 (2001).

[9] I. G. Bearden *et al.* (BRAHMS Collaboration), Pseudorapidity Distributions of Charged Particles from Au + Au Collisions at the Maximum RHIC Energy, $\sqrt{s_{NN}} = 200$ GeV, Phys. Rev. Lett. **88**, 202301 (2002).

[10] K. Adcox *et al.* (PHENIX Collaboration), Centrality Dependence of Charged Particle Multiplicity in Au-Au Collisions at $\sqrt{s_{NN}} = 130$ GeV, Phys. Rev. Lett. **86**, 3500 (2001).

[11] B. Alver *et al.* (PHOBOS Collaboration), Charged-particle multiplicity and pseudorapidity distributions measured with the PHOBOS detector in Au + Au, Cu + Cu, d + Au, and p + p collisions at ultrarelativistic energies, Phys. Rev. C **83**, 024913 (2011).

[12] B. I. Abelev *et al.* (STAR Collaboration), Systematic measurements of identified particle spectra in pp, d + Au, and Au + Au collisions at the STAR detector, Phys. Rev. C **79**, 034909 (2009).

[13] K. Aamodt *et al.* (ALICE Collaboration), The ALICE experiment at the CERN LHC, J. Instrum. **3**, S08002 (2008).

[14] B. Abelev *et al.* (ALICE Collaboration), Performance of the ALICE experiment at the CERN LHC, Int. J. Mod. Phys. A **29**, 1430044 (2014).

[15] ALICE Collaboration, Technical Report No. ALICE-PUBLIC-2015-008, 2015, https://cds.cern.ch/record/2118084.

[16] B. Abelev *et al.* (ALICE Collaboration), Centrality determination of Pb-Pb collisions at $\sqrt{s_{NN}} = 2.76$ TeV with ALICE, Phys. Rev. C **88**, 044909 (2013).

[17] H. De Vries, C. W. De Jager, and C. De Vries, Nuclear charge-density-distribution parameters from elastic electron scattering, At. Data Nucl. Data Tables **36**, 495 (1987).

[18] B. Abelev *et al.* (ALICE Collaboration), Pseudorapidity Density of Charged Particles in p + Pb Collisions at $\sqrt{s_{NN}} = 5.02$ TeV, Phys. Rev. Lett. **110**, 032301 (2013).

[19] K. Aamodt *et al.* (ALICE Collaboration), Charged-Particle Multiplicity Density at Mid-Rapidity in Central Pb-Pb Collisions at $\sqrt{s_{NN}} = 2.76$ TeV, Phys. Rev. Lett. **105**, 252301 (2010).

[20] X.-N. Wang and M. Gyulassy, HIJING: A Monte Carlo model for multiple jet production in pp, p A, and A A collisions, Phys. Rev. D **44**, 3501 (1991).

[21] R. Brun *et al.*, CERN Program Library Long Write-up No. W5013, 1994.

[22] B. Abelev *et al.* (ALICE Collaboration), Centrality dependence of charged particle production at large transverse momentum in Pb-Pb collisions at $\sqrt{s_{\mathrm{NN}}} = 2.76$ TeV, Phys. Lett. B **720**, 52 (2013).

[23] B. Abelev *et al.* (ALICE Collaboration), Centrality dependence of π, K, and p production in Pb-Pb collisions at $\sqrt{s_{NN}} = 2.76$ TeV, Phys. Rev. C **88**, 044910 (2013).

[24] B. Abelev *et al.* (ALICE Collaboration), K^0_S and Λ Production in Pb-Pb Collisions at $\sqrt{s_{NN}} = 2.76$ TeV, Phys. Rev. Lett. **111**, 222301 (2013).

[25] B. Abelev *et al.* (ALICE Collaboration), Multi-strange baryon production at mid-rapidity in Pb-Pb collisions at $\sqrt{s_{\mathrm{NN}}} = 2.76$ TeV, Phys. Lett. B **728**, 216 (2014); **734**, 409 (E) (2014).

[26] K. Aamodt *et al.* (ALICE Collaboration), Charged-particle multiplicities in proton-proton collisions at $\sqrt{s} = 0.9$ to 8 TeV, arXiv:1509.07541.

[27] V. Khachatryan *et al.* (CMS Collaboration), Pseudorapidity distribution of charged hadrons in proton-proton collisions at $\sqrt{s} = 13$ TeV, Phys. Lett. B **751**, 143 (2015).

[28] J. Adam *et al.* (ALICE Collaboration), Pseudorapidity and transverse-momentum distributions of charged particles in

proton-proton collisions at $\sqrt{s} = 13$ TeV, Phys. Lett. B **753**, 319 (2016).
[29] B. Abelev *et al.* (ALICE Collaboration), Pseudorapidity Density of Charged Particles in $p+\mathrm{Pb}$ Collisions at $\sqrt{s_{NN}} = 5.02$ TeV, Phys. Rev. Lett. **110**, 032301 (2013).
[30] B. B. Back *et al.* (PHOBOS Collaboration), Pseudorapidity Distribution of Charged Particles in $d+\mathrm{Au}$ Collisions at $\sqrt{s_{NN}} = 200$ GeV, Phys. Rev. Lett. **93**, 082301 (2004).
[31] H. Niemi, K. J. Eskola, and R. Paatelainen, Event-by-event fluctuations in a perturbative QCD + saturation + hydrodynamics model: Determining QCD matter shear viscosity in ultrarelativistic heavy-ion collisions, Phys. Rev. C **93**, 024907 (2016).
[32] H. Niemi, K. J. Eskola, R. Paatelainen, and K. Tuominen, Predictions for 5.023 TeV $\mathrm{Pb}+\mathrm{Pb}$ collisions at the CERN Large Hadron Collider, Phys. Rev. C **93**, 014912 (2016).
[33] W.-T. Deng, X.-N. Wang, and R. Xu, Hadron production in $p+p$, $p+\mathrm{Pb}$, and $\mathrm{Pb}+\mathrm{Pb}$ collisions with the HIJING 2.0 model at energies available at the CERN Large Hadron Collider, Phys. Rev. C **83**, 014915 (2011).
[34] A. Dumitru, D. E. Kharzeev, E. M. Levin, and Y. Nara, Gluon saturation in pA collisions at energies available at the CERN Large Hadron Collider: Predictions for hadron multiplicities, Phys. Rev. C **85**, 044920 (2012).
[35] J. L. Albacete, A. Dumitru, and Y. Nara, CGC initial conditions at RHIC and LHC, J. Phys. Conf. Ser. **316**, 012011 (2011).
[36] J. L. Albacete and A. Dumitru, A model for gluon production in heavy-ion collisions at the LHC with rcBK unintegrated gluon densities, arXiv:1011.5161.
[37] N. Armesto, C. A. Salgado, and U. A. Wiedemann, Relating High-Energy Lepton-Hadron, Proton-Nucleus and Nucleus-Nucleus Collisions through Geometric Scaling, Phys. Rev. Lett. **94**, 022002 (2005).
[38] D. Kharzeev, E. Levin, and M. Nardi, Color glass condensate at the LHC: Hadron multiplicities in pp, pA, and AA collisions, Nucl. Phys. **A747**, 609 (2005).
[39] T. Pierog, I. Karpenko, J. M. Katzy, E. Yatsenko, and K. Werner, EPOS LHC: Test of collective hadronization with data measured at the CERN Large Hadron Collider, Phys. Rev. C **92**, 034906 (2015).
[40] I. Helenius, K. J. Eskola, H. Honkanen, and C. A. Salgado, Impact-parameter dependent nuclear parton distribution functions: EPS09s and EKS98s and their applications in nuclear hard processes, J. High Energy Phys. 07 (2012) 073.

J. Adam,[40] D. Adamová,[84] M. M. Aggarwal,[88] G. Aglieri Rinella,[36] M. Agnello,[110] N. Agrawal,[48] Z. Ahammed,[132] S. Ahmad,[19] S. U. Ahn,[68] S. Aiola,[136] A. Akindinov,[58] S. N. Alam,[132] D. Aleksandrov,[80] B. Alessandro,[110] D. Alexandre,[101] R. Alfaro Molina,[64] A. Alici,[12,104] A. Alkin,[3] J. R. M. Almaraz,[119] J. Alme,[38] T. Alt,[43] S. Altinpinar,[18] I. Altsybeev,[131] C. Alves Garcia Prado,[120] C. Andrei,[78] A. Andronic,[97] V. Anguelov,[94] T. Antičić,[98] F. Antinori,[107] P. Antonioli,[104] L. Aphecetche,[113] H. Appelshäuser,[53] S. Arcelli,[28] R. Arnaldi,[110] O. W. Arnold,[37,93] I. C. Arsene,[22] M. Arslandok,[53] B. Audurier,[113] A. Augustinus,[36] R. Averbeck,[97] M. D. Azmi,[19] A. Badalà,[106] Y. W. Baek,[67] S. Bagnasco,[110] R. Bailhache,[53] R. Bala,[91] S. Balasubramanian,[136] A. Baldisseri,[15] R. C. Baral,[61] A. M. Barbano,[27] R. Barbera,[29] F. Barile,[33] G. G. Barnaföldi,[135] L. S. Barnby,[101] V. Barret,[70] P. Bartalini,[7] K. Barth,[36] J. Bartke,[117] E. Bartsch,[53] M. Basile,[28] N. Bastid,[70] S. Basu,[132] B. Bathen,[54] G. Batigne,[113] A. Batista Camejo,[70] B. Batyunya,[66] P. C. Batzing,[22] I. G. Bearden,[81] H. Beck,[53] C. Bedda,[110] N. K. Behera,[50] I. Belikov,[55] F. Bellini,[28] H. Bello Martinez,[2] R. Bellwied,[122] R. Belmont,[134] E. Belmont-Moreno,[64] V. Belyaev,[75] P. Benacek,[84] G. Bencedi,[135] S. Beole,[27] I. Berceanu,[78] A. Bercuci,[78] Y. Berdnikov,[86] D. Berenyi,[135] R. A. Bertens,[57] D. Berzano,[36] L. Betev,[36] A. Bhasin,[91] I. R. Bhat,[91] A. K. Bhati,[88] B. Bhattacharjee,[45] J. Bhom,[128] L. Bianchi,[122] N. Bianchi,[72] C. Bianchin,[134,57] J. Bielčík,[40] J. Bielčíková,[84] A. Bilandzic,[81,37,93] G. Biro,[135] R. Biswas,[4] S. Biswas,[79] S. Bjelogrlic,[57] J. T. Blair,[118] D. Blau,[80] C. Blume,[53] F. Bock,[74,94] A. Bogdanov,[75] H. Bøggild,[81] L. Boldizsár,[135] M. Bombara,[41] J. Book,[53] H. Borel,[15] A. Borissov,[96] M. Borri,[83,124] F. Bossú,[65] E. Botta,[27] C. Bourjau,[81] P. Braun-Munzinger,[97] M. Bregant,[120] T. Breitner,[52] T. A. Broker,[53] T. A. Browning,[95] M. Broz,[40] E. J. Brucken,[46] E. Bruna,[110] G. E. Bruno,[33] D. Budnikov,[99] H. Buesching,[53] S. Bufalino,[36,27] P. Buncic,[36] O. Busch,[94,128] Z. Buthelezi,[65] J. B. Butt,[16] J. T. Buxton,[20] D. Caffarri,[36] X. Cai,[7] H. Caines,[136] L. Calero Diaz,[72] A. Caliva,[57] E. Calvo Villar,[102] P. Camerini,[26] F. Carena,[36] W. Carena,[36] F. Carnesecchi,[28] J. Castillo Castellanos,[15] A. J. Castro,[125] E. A. R. Casula,[25] C. Ceballos Sanchez,[9] P. Cerello,[110] J. Cerkala,[115] B. Chang,[123] S. Chapeland,[36] M. Chartier,[124] J. L. Charvet,[15] S. Chattopadhyay,[132] S. Chattopadhyay,[100] A. Chauvin,[93,37] V. Chelnokov,[3] M. Cherney,[87] C. Cheshkov,[130] B. Cheynis,[130] V. Chibante Barroso,[36] D. D. Chinellato,[121] S. Cho,[50] P. Chochula,[36] K. Choi,[96] M. Chojnacki,[81] S. Choudhury,[132] P. Christakoglou,[82] C. H. Christensen,[81] P. Christiansen,[34] T. Chujo,[128] S. U. Chung,[96] C. Cicalo,[105] L. Cifarelli,[12,28] F. Cindolo,[104] J. Cleymans,[90] F. Colamaria,[33] D. Colella,[59,36] A. Collu,[74,25] M. Colocci,[28] G. Conesa Balbastre,[71] Z. Conesa del Valle,[51] M. E. Connors,[136,a] J. G. Contreras,[40] T. M. Cormier,[85] Y. Corrales Morales,[110] I. Cortés Maldonado,[2] P. Cortese,[32] M. R. Cosentino,[120] F. Costa,[36] P. Crochet,[70] R. Cruz Albino,[11] E. Cuautle,[63] L. Cunqueiro,[54,36] T. Dahms,[93,37]

A. Dainese,[107] M. C. Danisch,[94] A. Danu,[62] D. Das,[100] I. Das,[100,51] S. Das,[4] A. Dash,[121,79] S. Dash,[48] S. De,[120] A. De Caro,[12,31] G. de Cataldo,[103] C. de Conti,[120] J. de Cuveland,[43] A. De Falco,[25] D. De Gruttola,[12,31] N. De Marco,[110] S. De Pasquale,[31] A. Deisting,[97,94] A. Deloff,[77] E. Dénes,[135,†] C. Deplano,[82] P. Dhankher,[48] D. Di Bari,[33] A. Di Mauro,[36] P. Di Nezza,[72] M. A. Diaz Corchero,[10] T. Dietel,[90] P. Dillenseger,[53] R. Divià,[36] Ø. Djuvsland,[18] A. Dobrin,[62,82] D. Domenicis Gimenez,[120] B. Dönigus,[53] O. Dordic,[22] T. Drozhzhova,[53] A. K. Dubey,[132] A. Dubla,[57] L. Ducroux,[130] P. Dupieux,[70] R. J. Ehlers,[136] D. Elia,[103] E. Endress,[102] H. Engel,[52] E. Epple,[136] B. Erazmus,[113] I. Erdemir,[53] F. Erhardt,[129] B. Espagnon,[51] M. Estienne,[113] S. Esumi,[128] J. Eum,[96] D. Evans,[101] S. Evdokimov,[111] G. Eyyubova,[40] L. Fabbietti,[93,37] D. Fabris,[107] J. Faivre,[71] A. Fantoni,[72] M. Fasel,[74] L. Feldkamp,[54] A. Feliciello,[110] G. Feofilov,[131] J. Ferencei,[84] A. Fernández Téllez,[2] E. G. Ferreiro,[17] A. Ferretti,[27] A. Festanti,[30] V. J. G. Feuillard,[15,70] J. Figiel,[117] M. A. S. Figueredo,[124,120] S. Filchagin,[99] D. Finogeev,[56] F. M. Fionda,[25] E. M. Fiore,[33] M. G. Fleck,[94] M. Floris,[36] S. Foertsch,[65] P. Foka,[97] S. Fokin,[80] E. Fragiacomo,[109] A. Francescon,[36,30] U. Frankenfeld,[97] G. G. Fronze,[27] U. Fuchs,[36] C. Furget,[71] A. Furs,[56] M. Fusco Girard,[31] J. J. Gaardhøje,[81] M. Gagliardi,[27] A. M. Gago,[102] M. Gallio,[27] D. R. Gangadharan,[74] P. Ganoti,[89] C. Gao,[7] C. Garabatos,[97] E. Garcia-Solis,[13] C. Gargiulo,[36] P. Gasik,[93,37] E. F. Gauger,[118] M. Germain,[113] A. Gheata,[36] M. Gheata,[36,62] P. Ghosh,[132] S. K. Ghosh,[4] P. Gianotti,[72] P. Giubellino,[110,36] P. Giubilato,[30] E. Gladysz-Dziadus,[117] P. Glässel,[94] D. M. Goméz Coral,[64] A. Gomez Ramirez,[52] V. Gonzalez,[10] P. González-Zamora,[10] S. Gorbunov,[43] L. Görlich,[117] S. Gotovac,[116] V. Grabski,[64] O. A. Grachov,[136] L. K. Graczykowski,[133] K. L. Graham,[101] A. Grelli,[57] A. Grigoras,[36] C. Grigoras,[36] V. Grigoriev,[75] A. Grigoryan,[1] S. Grigoryan,[66] B. Grinyov,[3] N. Grion,[109] J. M. Gronefeld,[97] J. F. Grosse-Oetringhaus,[36] J.-Y. Grossiord,[130] R. Grosso,[97] F. Guber,[56] R. Guernane,[71] B. Guerzoni,[28] K. Gulbrandsen,[81] T. Gunji,[127] A. Gupta,[91] R. Gupta,[91] R. Haake,[54] Ø. Haaland,[18] C. Hadjidakis,[51] M. Haiduc,[62] H. Hamagaki,[127] G. Hamar,[135] J. C. Hamon,[55] J. W. Harris,[136] A. Harton,[13] D. Hatzifotiadou,[104] S. Hayashi,[127] S. T. Heckel,[53] H. Helstrup,[38] A. Herghelegiu,[78] G. Herrera Corral,[11] B. A. Hess,[35] K. F. Hetland,[38] H. Hillemanns,[36] B. Hippolyte,[55] D. Horak,[40] R. Hosokawa,[128] P. Hristov,[36] M. Huang,[18] T. J. Humanic,[20] N. Hussain,[45] T. Hussain,[19] D. Hutter,[43] D. S. Hwang,[21] R. Ilkaev,[99] M. Inaba,[128] E. Incani,[25] M. Ippolitov,[75,80] M. Irfan,[19] M. Ivanov,[97] V. Ivanov,[86] V. Izucheev,[111] N. Jacazio,[28] P. M. Jacobs,[74] M. B. Jadhav,[48] S. Jadlovska,[115] J. Jadlovsky,[115,59] C. Jahnke,[120] M. J. Jakubowska,[133] H. J. Jang,[68] M. A. Janik,[133] P. H. S. Y. Jayarathna,[122] C. Jena,[30] S. Jena,[122] R. T. Jimenez Bustamante,[97] P. G. Jones,[101] A. Jusko,[101] P. Kalinak,[59] A. Kalweit,[36] J. Kamin,[53] J. H. Kang,[137] V. Kaplin,[75] S. Kar,[132] A. Karasu Uysal,[69] O. Karavichev,[56] T. Karavicheva,[56] L. Karayan,[97,94] E. Karpechev,[56] U. Kebschull,[52] R. Keidel,[138] D. L. D. Keijdener,[57] M. Keil,[36] M. Mohisin Khan,[19,b] P. Khan,[100] S. A. Khan,[132] A. Khanzadeev,[86] Y. Kharlov,[111] B. Kileng,[38] D. W. Kim,[44] D. J. Kim,[123] D. Kim,[137] H. Kim,[137] J. S. Kim,[44] M. Kim,[137] S. Kim,[21] T. Kim,[137] S. Kirsch,[43] I. Kisel,[43] S. Kiselev,[58] A. Kisiel,[133] G. Kiss,[135] J. L. Klay,[6] C. Klein,[53] J. Klein,[36] C. Klein-Bösing,[54] S. Klewin,[94] A. Kluge,[36] M. L. Knichel,[94] A. G. Knospe,[118] C. Kobdaj,[114] M. Kofarago,[36] T. Kollegger,[97] A. Kolojvari,[131] V. Kondratiev,[131] N. Kondratyeva,[75] E. Kondratyuk,[111] A. Konevskikh,[56] M. Kopcik,[115] P. Kostarakis,[89] M. Kour,[91] C. Kouzinopoulos,[36] O. Kovalenko,[77] V. Kovalenko,[131] M. Kowalski,[117] G. Koyithatta Meethaleveedu,[48] I. Králik,[59] A. Kravčáková,[41] M. Kretz,[43] M. Krivda,[59,101] F. Krizek,[84] E. Kryshen,[86,36] M. Krzewicki,[43] A. M. Kubera,[20] V. Kučera,[84] C. Kuhn,[55] P. G. Kuijer,[82] A. Kumar,[91] J. Kumar,[48] L. Kumar,[88] S. Kumar,[48] P. Kurashvili,[77] A. Kurepin,[56] A. B. Kurepin,[56] A. Kuryakin,[99] M. J. Kweon,[50] Y. Kwon,[137] S. L. La Pointe,[110] P. La Rocca,[29] P. Ladron de Guevara,[11] C. Lagana Fernandes,[120] I. Lakomov,[36] R. Langoy,[42] C. Lara,[52] A. Lardeux,[15] A. Lattuca,[27] E. Laudi,[36] R. Lea,[26] L. Leardini,[94] G. R. Lee,[101] S. Lee,[137] F. Lehas,[82] R. C. Lemmon,[83] V. Lenti,[103] E. Leogrande,[57] I. León Monzón,[119] H. León Vargas,[64] M. Leoncino,[27] P. Lévai,[135] S. Li,[7,70] X. Li,[14] J. Lien,[42] R. Lietava,[101] S. Lindal,[22] V. Lindenstruth,[43] C. Lippmann,[97] M. A. Lisa,[20] H. M. Ljunggren,[34] D. F. Lodato,[57] P. I. Loenne,[18] V. Loginov,[75] C. Loizides,[74] X. Lopez,[70] E. López Torres,[9] A. Lowe,[135] P. Luettig,[53] M. Lunardon,[30] G. Luparello,[26] T. H. Lutz,[136] A. Maevskaya,[56] M. Mager,[36] S. Mahajan,[91] S. M. Mahmood,[22] A. Maire,[55] R. D. Majka,[136] M. Malaev,[86] I. Maldonado Cervantes,[63] L. Malinina,[66,c] D. Mal'Kevich,[58] P. Malzacher,[97] A. Mamonov,[99] V. Manko,[80] F. Manso,[70] V. Manzari,[36,103] M. Marchisone,[27,65,126] J. Mareš,[60] G. V. Margagliotti,[26] A. Margotti,[104] J. Margutti,[57] A. Marín,[97] C. Markert,[118] M. Marquard,[53] N. A. Martin,[97] J. Martin Blanco,[113] P. Martinengo,[36] M. I. Martínez,[2] G. Martínez García,[113] M. Martinez Pedreira,[36] A. Mas,[120] S. Masciocchi,[97] M. Masera,[27] A. Masoni,[105] L. Massacrier,[113] A. Mastroserio,[33] A. Matyja,[117] C. Mayer,[117,36] J. Mazer,[125] M. A. Mazzoni,[108] D. Mcdonald,[122] F. Meddi,[24] Y. Melikyan,[75] A. Menchaca-Rocha,[64] E. Meninno,[31] J. Mercado Pérez,[94] M. Meres,[39] Y. Miake,[128] M. M. Mieskolainen,[46] K. Mikhaylov,[66,58] L. Milano,[74,36] J. Milosevic,[22] L. M. Minervini,[103,23] A. Mischke,[57] A. N. Mishra,[49] D. Miśkowiec,[97] J. Mitra,[132] C. M. Mitu,[62] N. Mohammadi,[57] B. Mohanty,[79,132]

L. Molnar,[55,113] L. Montaño Zetina,[11] E. Montes,[10] D. A. Moreira De Godoy,[113,54] L. A. P. Moreno,[2] S. Moretto,[30] A. Morreale,[113] A. Morsch,[36] V. Muccifora,[72] E. Mudnic,[116] D. Mühlheim,[54] S. Muhuri,[132] M. Mukherjee,[132] J. D. Mulligan,[136] M. G. Munhoz,[120] R. H. Munzer,[37,93] H. Murakami,[127] S. Murray,[65] L. Musa,[36] J. Musinsky,[59] B. Naik,[48] R. Nair,[77] B. K. Nandi,[48] R. Nania,[104] E. Nappi,[103] M. U. Naru,[16] H. Natal da Luz,[120] C. Nattrass,[125] S. R. Navarro,[2] K. Nayak,[79] R. Nayak,[48] T. K. Nayak,[132] S. Nazarenko,[99] A. Nedosekin,[58] L. Nellen,[63] F. Ng,[122] M. Nicassio,[97] M. Niculescu,[62] J. Niedziela,[36] B. S. Nielsen,[81] S. Nikolaev,[80] S. Nikulin,[80] V. Nikulin,[86] F. Noferini,[104,12] P. Nomokonov,[66] G. Nooren,[57] J. C. C. Noris,[2] J. Norman,[124] A. Nyanin,[80] J. Nystrand,[18] H. Oeschler,[94] S. Oh,[136] S. K. Oh,[67] A. Ohlson,[36] A. Okatan,[69] T. Okubo,[47] L. Olah,[135] J. Oleniacz,[133] A. C. Oliveira Da Silva,[120] M. H. Oliver,[136] J. Onderwaater,[97] C. Oppedisano,[110] R. Orava,[46] A. Ortiz Velasquez,[63] A. Oskarsson,[34] J. Otwinowski,[117] K. Oyama,[94,76] M. Ozdemir,[53] Y. Pachmayer,[94] P. Pagano,[31] G. Paić,[63] S. K. Pal,[132] J. Pan,[134] A. K. Pandey,[48] V. Papikyan,[1] G. S. Pappalardo,[106] P. Pareek,[49] W. J. Park,[97] S. Parmar,[88] A. Passfeld,[54] V. Paticchio,[103] R. N. Patra,[132] B. Paul,[100] H. Pei,[7] T. Peitzmann,[57] H. Pereira Da Costa,[15] D. Peresunko,[80,75] C. E. Pérez Lara,[82] E. Perez Lezama,[53] V. Peskov,[53] Y. Pestov,[5] V. Petráček,[40] V. Petrov,[111] M. Petrovici,[78] C. Petta,[29] S. Piano,[109] M. Pikna,[39] P. Pillot,[113] L. O. D. L. Pimentel,[81] O. Pinazza,[36,104] L. Pinsky,[122] D. B. Piyarathna,[122] M. Płoskoń,[74] M. Planinic,[129] J. Pluta,[133] S. Pochybova,[135] P. L. M. Podesta-Lerma,[119] M. G. Poghosyan,[85,87] B. Polichtchouk,[111] N. Poljak,[129] W. Poonsawat,[114] A. Pop,[78] S. Porteboeuf-Houssais,[70] J. Porter,[74] J. Pospisil,[84] S. K. Prasad,[4] R. Preghenella,[104,36] F. Prino,[110] C. A. Pruneau,[134] I. Pshenichnov,[56] M. Puccio,[27] G. Puddu,[25] P. Pujahari,[134] V. Punin,[99] J. Putschke,[134] H. Qvigstad,[22] A. Rachevski,[109] S. Raha,[4] S. Rajput,[91] J. Rak,[123] A. Rakotozafindrabe,[15] L. Ramello,[32] F. Rami,[55] R. Raniwala,[92] S. Raniwala,[92] S. S. Räsänen,[46] B. T. Rascanu,[53] D. Rathee,[88] K. F. Read,[125,85] K. Redlich,[77] R. J. Reed,[134] A. Rehman,[18] P. Reichelt,[53] F. Reidt,[94,36] X. Ren,[7] R. Renfordt,[53] A. R. Reolon,[72] A. Reshetin,[56] J.-P. Revol,[12] K. Reygers,[94] V. Riabov,[86] R. A. Ricci,[73] T. Richert,[34] M. Richter,[22] P. Riedler,[36] W. Riegler,[36] F. Riggi,[29] C. Ristea,[62] E. Rocco,[57] M. Rodríguez Cahuantzi,[2,11] A. Rodriguez Manso,[82] K. Røed,[22] E. Rogochaya,[66] D. Rohr,[43] D. Röhrich,[18] R. Romita,[124] F. Ronchetti,[72,36] L. Ronflette,[113] P. Rosnet,[70] A. Rossi,[30,36] F. Roukoutakis,[89] A. Roy,[49] C. Roy,[55] P. Roy,[100] A. J. Rubio Montero,[10] R. Rui,[26] R. Russo,[27] E. Ryabinkin,[80] Y. Ryabov,[86] A. Rybicki,[117] S. Sadovsky,[111] K. Šafařík,[36] B. Sahlmuller,[53] P. Sahoo,[49] R. Sahoo,[49] S. Sahoo,[61] P. K. Sahu,[61] J. Saini,[132] S. Sakai,[72] M. A. Saleh,[134] J. Salzwedel,[20] S. Sambyal,[91] V. Samsonov,[86] L. Šándor,[59] A. Sandoval,[64] M. Sano,[128] D. Sarkar,[132] P. Sarma,[45] E. Scapparone,[104] F. Scarlassara,[30] C. Schiaua,[78] R. Schicker,[94] C. Schmidt,[97] H. R. Schmidt,[35] S. Schuchmann,[53] J. Schukraft,[36] M. Schulc,[40] T. Schuster,[136] Y. Schutz,[36,113] K. Schwarz,[97] K. Schweda,[97] G. Scioli,[28] E. Scomparin,[110] R. Scott,[125] M. Šefčík,[41] J. E. Seger,[87] Y. Sekiguchi,[127] D. Sekihata,[47] I. Selyuzhenkov,[97] K. Senosi,[65] S. Senyukov,[3,36] E. Serradilla,[10,64] A. Sevcenco,[62] A. Shabanov,[56] A. Shabetai,[113] O. Shadura,[3] R. Shahoyan,[36] A. Shangaraev,[111] A. Sharma,[91] M. Sharma,[91] M. Sharma,[91] N. Sharma,[125] K. Shigaki,[47] K. Shtejer,[9,27] Y. Sibiriak,[80] S. Siddhanta,[105] K. M. Sielewicz,[36] T. Siemiarczuk,[77] D. Silvermyr,[34] C. Silvestre,[71] G. Simatovic,[129] G. Simonetti,[36] R. Singaraju,[132] R. Singh,[79] S. Singha,[132,79] V. Singhal,[132] B. C. Sinha,[132] T. Sinha,[100] B. Sitar,[39] M. Sitta,[32] T. B. Skaali,[22] M. Slupecki,[123] N. Smirnov,[136] R. J. M. Snellings,[57] T. W. Snellman,[123] C. Søgaard,[34] J. Song,[96] M. Song,[137] Z. Song,[7] F. Soramel,[30] S. Sorensen,[125] R. D. de Souza,[121] F. Sozzi,[97] M. Spacek,[40] E. Spiriti,[72] I. Sputowska,[117] M. Spyropoulou-Stassinaki,[89] J. Stachel,[94] I. Stan,[62] P. Stankus,[85] G. Stefanek,[77] E. Stenlund,[34] G. Steyn,[65] J. H. Stiller,[94] D. Stocco,[113] P. Strmen,[39] A. A. P. Suaide,[120] T. Sugitate,[47] C. Suire,[51] M. Suleymanov,[16] M. Suljic,[26,†] R. Sultanov,[58] M. Šumbera,[84] A. Szabo,[39] A. Szanto de Toledo,[120,†] I. Szarka,[39] A. Szczepankiewicz,[36] M. Szymanski,[133] U. Tabassam,[16] J. Takahashi,[121] G. J. Tambave,[18] N. Tanaka,[128] M. A. Tangaro,[33] M. Tarhini,[51] M. Tariq,[19] M. G. Tarzila,[78] A. Tauro,[36] G. Tejeda Muñoz,[2] A. Telesca,[36] K. Terasaki,[127] C. Terrevoli,[30] B. Teyssier,[130] J. Thäder,[74] D. Thomas,[118] R. Tieulent,[130] A. R. Timmins,[122] A. Toia,[53] S. Trogolo,[27] G. Trombetta,[33] V. Trubnikov,[3] W. H. Trzaska,[123] T. Tsuji,[127] A. Tumkin,[99] R. Turrisi,[107] T. S. Tveter,[22] K. Ullaland,[18] A. Uras,[130] G. L. Usai,[25] A. Utrobicic,[129] M. Vajzer,[84] M. Vala,[59] L. Valencia Palomo,[70] S. Vallero,[27] J. Van Der Maarel,[57] J. W. Van Hoorne,[36] M. van Leeuwen,[57] T. Vanat,[84] P. Vande Vyvre,[36] D. Varga,[135] A. Vargas,[2] M. Vargyas,[123] R. Varma,[48] M. Vasileiou,[89] A. Vasiliev,[80] A. Vauthier,[71] V. Vechernin,[131] A. M. Veen,[57] M. Veldhoen,[57] A. Velure,[18] M. Venaruzzo,[73] E. Vercellin,[27] S. Vergara Limón,[2] R. Vernet,[8] M. Verweij,[134] L. Vickovic,[116] G. Viesti,[30,†] J. Viinikainen,[123] Z. Vilakazi,[126] O. Villalobos Baillie,[101] A. Villatoro Tello,[2] A. Vinogradov,[80] L. Vinogradov,[131] Y. Vinogradov,[99,†] T. Virgili,[31] V. Vislavicius,[34] Y. P. Viyogi,[132] A. Vodopyanov,[66] M. A. Völkl,[94] K. Voloshin,[58] S. A. Voloshin,[134] G. Volpe,[33] B. von Haller,[36] I. Vorobyev,[37,93] D. Vranic,[97,36] J. Vrláková,[41] B. Vulpescu,[70] B. Wagner,[18] J. Wagner,[97] H. Wang,[57] M. Wang,[7,113] D. Watanabe,[128] Y. Watanabe,[127] M. Weber,[36,112] S. G. Weber,[97] D. F. Weiser,[94] J. P. Wessels,[54] U. Westerhoff,[54] A. M. Whitehead,[90] J. Wiechula,[35] J. Wikne,[22] G. Wilk,[77]

J. Wilkinson,[94] M. C. S. Williams,[104] B. Windelband,[94] M. Winn,[94] H. Yang,[57] P. Yang,[7] S. Yano,[47] C. Yasar,[69] Z. Yin,[7] H. Yokoyama,[128] I.-K. Yoo,[96] J. H. Yoon,[50] V. Yurchenko,[3] I. Yushmanov,[80] A. Zaborowska,[133] V. Zaccolo,[81] A. Zaman,[16] C. Zampolli,[36,104] H. J. C. Zanoli,[120] S. Zaporozhets,[66] N. Zardoshti,[101] A. Zarochentsev,[131] P. Závada,[60] N. Zaviyalov,[99] H. Zbroszczyk,[133] I. S. Zgura,[62] M. Zhalov,[86] H. Zhang,[18] X. Zhang,[74] Y. Zhang,[7] C. Zhang,[57] Z. Zhang,[7] C. Zhao,[22] N. Zhigareva,[58] D. Zhou,[7] Y. Zhou,[81] Z. Zhou,[18] H. Zhu,[18] J. Zhu,[113,7] A. Zichichi,[28,12] A. Zimmermann,[94] M. B. Zimmermann,[54,36] G. Zinovjev[3] and M. Zyzak[43]

(ALICE Collaboration)

[1]*A.I. Alikhanyan National Science Laboratory (Yerevan Physics Institute) Foundation, Yerevan, Armenia*
[2]*Benemérita Universidad Autónoma de Puebla, Puebla, Mexico*
[3]*Bogolyubov Institute for Theoretical Physics, Kiev, Ukraine*
[4]*Bose Institute, Department of Physics and Centre for Astroparticle Physics and Space Science (CAPSS), Kolkata, India*
[5]*Budker Institute for Nuclear Physics, Novosibirsk, Russia*
[6]*California Polytechnic State University, San Luis Obispo, California, USA*
[7]*Central China Normal University, Wuhan, China*
[8]*Centre de Calcul de l'IN2P3, Villeurbanne, France*
[9]*Centro de Aplicaciones Tecnológicas y Desarrollo Nuclear (CEADEN), Havana, Cuba*
[10]*Centro de Investigaciones Energéticas Medioambientales y Tecnológicas (CIEMAT), Madrid, Spain*
[11]*Centro de Investigación y de Estudios Avanzados (CINVESTAV), Mexico City and Mérida, Mexico*
[12]*Centro Fermi - Museo Storico della Fisica e Centro Studi e Ricerche "Enrico Fermi", Rome, Italy*
[13]*Chicago State University, Chicago, Illinois, USA*
[14]*China Institute of Atomic Energy, Beijing, China*
[15]*Commissariat à l'Energie Atomique, IRFU, Saclay, France*
[16]*COMSATS Institute of Information Technology (CIIT), Islamabad, Pakistan*
[17]*Departamento de Física de Partículas and IGFAE, Universidad de Santiago de Compostela, Santiago de Compostela, Spain*
[18]*Department of Physics and Technology, University of Bergen, Bergen, Norway*
[19]*Department of Physics, Aligarh Muslim University, Aligarh, India*
[20]*Department of Physics, Ohio State University, Columbus, Ohio, USA*
[21]*Department of Physics, Sejong University, Seoul, South Korea*
[22]*Department of Physics, University of Oslo, Oslo, Norway*
[23]*Dipartimento di Elettrotecnica ed Elettronica del Politecnico, Bari, Italy*
[24]*Dipartimento di Fisica dell'Università "La Sapienza" and Sezione INFN Rome, Italy*
[25]*Dipartimento di Fisica dell'Università and Sezione INFN, Cagliari, Italy*
[26]*Dipartimento di Fisica dell'Università and Sezione INFN, Trieste, Italy*
[27]*Dipartimento di Fisica dell'Università and Sezione INFN, Turin, Italy*
[28]*Dipartimento di Fisica e Astronomia dell'Università and Sezione INFN, Bologna, Italy*
[29]*Dipartimento di Fisica e Astronomia dell'Università and Sezione INFN, Catania, Italy*
[30]*Dipartimento di Fisica e Astronomia dell'Università and Sezione INFN, Padova, Italy*
[31]*Dipartimento di Fisica "E. R. Caianiello" dell'Università and Gruppo Collegato INFN, Salerno, Italy*
[32]*Dipartimento di Scienze e Innovazione Tecnologica dell'Università del Piemonte Orientale and Gruppo Collegato INFN, Alessandria, Italy*
[33]*Dipartimento Interateneo di Fisica "M. Merlin" and Sezione INFN, Bari, Italy*
[34]*Division of Experimental High Energy Physics, University of Lund, Lund, Sweden*
[35]*Eberhard Karls Universität Tübingen, Tübingen, Germany*
[36]*European Organization for Nuclear Research (CERN), Geneva, Switzerland*
[37]*Excellence Cluster Universe, Technische Universität München, Munich, Germany*
[38]*Faculty of Engineering, Bergen University College, Bergen, Norway*
[39]*Faculty of Mathematics, Physics and Informatics, Comenius University, Bratislava, Slovakia*
[40]*Faculty of Nuclear Sciences and Physical Engineering, Czech Technical University in Prague, Prague, Czech Republic*
[41]*Faculty of Science, P. J. Šafárik University, Košice, Slovakia*
[42]*Faculty of Technology, Buskerud and Vestfold University College, Vestfold, Norway*
[43]*Frankfurt Institute for Advanced Studies, Johann Wolfgang Goethe-Universität Frankfurt, Frankfurt, Germany*
[44]*Gangneung-Wonju National University, Gangneung, South Korea*
[45]*Gauhati University, Department of Physics, Guwahati, India*
[46]*Helsinki Institute of Physics (HIP), Helsinki, Finland*
[47]*Hiroshima University, Hiroshima, Japan*
[48]*Indian Institute of Technology Bombay (IIT), Mumbai, India*

[49]Indian Institute of Technology Indore, Indore (IITI), India
[50]Inha University, Incheon, South Korea
[51]Institut de Physique Nucléaire d'Orsay (IPNO), Université Paris-Sud, CNRS-IN2P3, Orsay, France
[52]Institut für Informatik, Johann Wolfgang Goethe-Universität Frankfurt, Frankfurt, Germany
[53]Institut für Kernphysik, Johann Wolfgang Goethe-Universität Frankfurt, Frankfurt, Germany
[54]Institut für Kernphysik, Westfälische Wilhelms-Universität Münster, Münster, Germany
[55]Institut Pluridisciplinaire Hubert Curien (IPHC), Université de Strasbourg, CNRS-IN2P3, Strasbourg, France
[56]Institute for Nuclear Research, Academy of Sciences, Moscow, Russia
[57]Institute for Subatomic Physics of Utrecht University, Utrecht, Netherlands
[58]Institute for Theoretical and Experimental Physics, Moscow, Russia
[59]Institute of Experimental Physics, Slovak Academy of Sciences, Košice, Slovakia
[60]Institute of Physics, Academy of Sciences of the Czech Republic, Prague, Czech Republic
[61]Institute of Physics, Bhubaneswar, India
[62]Institute of Space Science (ISS), Bucharest, Romania
[63]Instituto de Ciencias Nucleares, Universidad Nacional Autónoma de México, Mexico City, Mexico
[64]Instituto de Física, Universidad Nacional Autónoma de México, Mexico City, Mexico
[65]iThemba LABS, National Research Foundation, Somerset West, South Africa
[66]Joint Institute for Nuclear Research (JINR), Dubna, Russia
[67]Konkuk University, Seoul, South Korea
[68]Korea Institute of Science and Technology Information, Daejeon, South Korea
[69]KTO Karatay University, Konya, Turkey
[70]Laboratoire de Physique Corpusculaire (LPC), Clermont Université,
Université Blaise Pascal, CNRS-IN2P3, Clermont-Ferrand, France
[71]Laboratoire de Physique Subatomique et de Cosmologie, Université Grenoble-Alpes, CNRS-IN2P3, Grenoble, France
[72]Laboratori Nazionali di Frascati, INFN, Frascati, Italy
[73]Laboratori Nazionali di Legnaro, INFN, Legnaro, Italy
[74]Lawrence Berkeley National Laboratory, Berkeley, California, USA
[75]Moscow Engineering Physics Institute, Moscow, Russia
[76]Nagasaki Institute of Applied Science, Nagasaki, Japan
[77]National Centre for Nuclear Studies, Warsaw, Poland
[78]National Institute for Physics and Nuclear Engineering, Bucharest, Romania
[79]National Institute of Science Education and Research, Bhubaneswar, India
[80]National Research Centre Kurchatov Institute, Moscow, Russia
[81]Niels Bohr Institute, University of Copenhagen, Copenhagen, Denmark
[82]Nikhef, Nationaal instituut voor subatomaire fysica, Amsterdam, Netherlands
[83]Nuclear Physics Group, STFC Daresbury Laboratory, Daresbury, United Kingdom
[84]Nuclear Physics Institute, Academy of Sciences of the Czech Republic, Řež u Prahy, Czech Republic
[85]Oak Ridge National Laboratory, Oak Ridge, Tennessee, USA
[86]Petersburg Nuclear Physics Institute, Gatchina, Russia
[87]Physics Department, Creighton University, Omaha, Nebraska, USA
[88]Physics Department, Panjab University, Chandigarh, India
[89]Physics Department, University of Athens, Athens, Greece
[90]Physics Department, University of Cape Town, Cape Town, South Africa
[91]Physics Department, University of Jammu, Jammu, India
[92]Physics Department, University of Rajasthan, Jaipur, India
[93]Physik Department, Technische Universität München, Munich, Germany
[94]Physikalisches Institut, Ruprecht-Karls-Universität Heidelberg, Heidelberg, Germany
[95]Purdue University, West Lafayette, Indiana, USA
[96]Pusan National University, Pusan, South Korea
[97]Research Division and ExtreMe Matter Institute EMMI,
GSI Helmholtzzentrum für Schwerionenforschung, Darmstadt, Germany
[98]Rudjer Bošković Institute, Zagreb, Croatia
[99]Russian Federal Nuclear Center (VNIIEF), Sarov, Russia
[100]Saha Institute of Nuclear Physics, Kolkata, India
[101]School of Physics and Astronomy, University of Birmingham, Birmingham, United Kingdom
[102]Sección Física, Departamento de Ciencias, Pontificia Universidad Católica del Perú, Lima, Peru
[103]Sezione INFN, Bari, Italy
[104]Sezione INFN, Bologna, Italy
[105]Sezione INFN, Cagliari, Italy
[106]Sezione INFN, Catania, Italy

[107]Sezione INFN, Padova, Italy
[108]Sezione INFN, Rome, Italy
[109]Sezione INFN, Trieste, Italy
[110]Sezione INFN, Turin, Italy
[111]SSC IHEP of NRC Kurchatov institute, Protvino, Russia
[112]Stefan Meyer Institut für Subatomare Physik (SMI), Vienna, Austria
[113]SUBATECH, Ecole des Mines de Nantes, Université de Nantes, CNRS-IN2P3, Nantes, France
[114]Suranaree University of Technology, Nakhon Ratchasima, Thailand
[115]Technical University of Košice, Košice, Slovakia
[116]Technical University of Split FESB, Split, Croatia
[117]The Henryk Niewodniczanski Institute of Nuclear Physics, Polish Academy of Sciences, Cracow, Poland
[118]The University of Texas at Austin, Physics Department, Austin, Texas, USA
[119]Universidad Autónoma de Sinaloa, Culiacán, Mexico
[120]Universidade de São Paulo (USP), São Paulo, Brazil
[121]Universidade Estadual de Campinas (UNICAMP), Campinas, Brazil
[122]University of Houston, Houston, Texas, USA
[123]University of Jyväskylä, Jyväskylä, Finland
[124]University of Liverpool, Liverpool, United Kingdom
[125]University of Tennessee, Knoxville, Tennessee, USA
[126]University of the Witwatersrand, Johannesburg, South Africa
[127]University of Tokyo, Tokyo, Japan
[128]University of Tsukuba, Tsukuba, Japan
[129]University of Zagreb, Zagreb, Croatia
[130]Université de Lyon, Université Lyon 1, CNRS/IN2P3, IPN-Lyon, Villeurbanne, France
[131]V. Fock Institute for Physics, St. Petersburg State University, St. Petersburg, Russia
[132]Variable Energy Cyclotron Centre, Kolkata, India
[133]Warsaw University of Technology, Warsaw, Poland
[134]Wayne State University, Detroit, Michigan, USA
[135]Wigner Research Centre for Physics, Hungarian Academy of Sciences, Budapest, Hungary
[136]Yale University, New Haven, Connecticut, USA
[137]Yonsei University, Seoul, South Korea
[138]Zentrum für Technologietransfer und Telekommunikation (ZTT), Fachhochschule Worms, Worms, Germany

[†]Deceased.
[a]Also at Georgia State University, Atlanta, GA, USA.
[b]Also at Department of Applied Physics, Aligarh Muslim University, Aligarh, India.
[c]Also at M.V. Lomonosov Moscow State University, D.V. Skobeltsyn Institute of Nuclear, Physics, Moscow, Russia.